Proc. Natl. Acad. Sci. USA
Vol. 91, pp. 5592–5596, June 1994
Medical Sciences

Granulocyte/macrophage colony-stimulating factor-deficient mice show no major perturbation of hematopoiesis but develop a characteristic pulmonary pathology

(hematopoietic growth factors/gene targeting/homologous recombination/pulmonary diseases)

EDOUARD STANLEY*†, GRAHAM J. LIESCHKE*, DIANNE GRAIL*, DONALD METCALF‡, GEORGE HODGSON*, JOHN A. M. GALL§, DARRYL W. MAHER*, JONATHAN CEBON*, VINCENT SINICKAS¶, AND ASHLEY R. DUNN*‖

*Ludwig Institute for Cancer Research, Melbourne Tumour Biology Branch, ‡Cancer Research Unit, Walter and Eliza Hall Institute of Medical Research, §Department of Anatomical Pathology, and ¶Department of Microbiology, Post Office, The Royal Melbourne Hospital, Victoria, 3050, Australia

Contributed by Donald Metcalf, February 14, 1994

ABSTRACT **Mice homozygous for a disrupted granulocyte/macrophage colony-stimulating factor (GM-CSF) gene develop normally and show no major perturbation of hematopoiesis up to 12 weeks of age. While most GM-CSF-deficient mice are superficially healthy and fertile, all develop abnormal lungs. There is extensive peribronchovascular infiltration with lymphocytes, predominantly B cells. Alveoli contain granular eosinophilic material and lamellar bodies, indicative of surfactant accumulation. There are numerous large intraalveolar phagocytic macrophages. Some mice have subclinical lung infections involving bacterial or fungal organisms, occasionally with focal areas of acute purulent inflammation or lobar pneumonia. Some features of this pathology resemble the human disorder alveolar proteinosis. These observations indicate that GM-CSF is not essential for the maintenance of normal levels of the major types of mature hematopoietic cells and their precursors in blood, marrow, and spleen. However, they implicate GM-CSF as essential for normal pulmonary physiology and resistance to local infection.**

Granulocyte/macrophage colony-stimulating factor (GM-CSF) is a hematopoietic growth factor that *in vitro* stimulates the survival, proliferation, differentiation, and function of myeloid cells and their precursors, particularly neutrophil and eosinophil granulocytes and monocyte/macrophages (for a review, see ref. 1). The *in vivo* effects of GM-CSF have been studied in murine models by injecting pharmacological doses of GM-CSF (2), by generating GM-CSF transgenic mice (3), and by reconstituting mice with marrow cells overproducing GM-CSF (4). These studies confirm the hematopoietic activity of GM-CSF *in vivo* and suggest that excess levels may be implicated in some disease processes. However, the usual physiological role of GM-CSF is not well defined (1, 5). We sought to define the physiological role of GM-CSF by generating GM-CSF-deficient mice through targeted disruption of the GM-CSF gene in embryonic stem cells. While GM-CSF-deficient mice have no major perturbation of hematopoiesis, they do have abnormal lungs, implicating GM-CSF as essential for normal pulmonary physiology.

MATERIALS AND METHODS

GM-CSF Targeting Vector and Isolation of Targeted Embryonal Stem (ES) Cell Clones. The GM-CSF targeting vector (Fig. 1) contained, from 5′ to 3′ in pIC20H, 900 bp of the GM-CSF gene promoter (*Rsa* I–*Sca* I) (6, 7), the *Escherichia coli lacZ* gene, a 700-bp fragment of the human β-globin gene 3′ untranslated region and a poly(A) addition motif (*Eco*RI–*Acc* I; gift of F. Grosveld, National Institute for Medical Research, London), the PGK-neo selectable marker (8), and approximately 10 kb of GM-CSF genomic sequence (7). The targeting vector was constructed to delete GM-CSF exons 1 and 2 and intron 1 between *Sca* I and *Sma* I sites. The linearized vector was electroporated into 129/OLA-derived E14 ES cells (9). Individual G418-resistant colonies were cloned and screened by PCR. The PCR primers were as follows (Fig. 1): **a**, 5′-CCAGCCTCAGAGACCCAGGTATCC-3′; **b**, 5′-GTTAGAGACGACTTCTACCTCTTC-3′; and **c**, a M13 (−47) 24-mer sequencing primer (New England Biolabs; no. 1224). In PCRs, primers **a** and **b** generate a 1.2-kb product from wild-type DNA, and **a** and **c** generate a 1.0-kb product from DNA containing a correctly integrated targeted construct. The reactant mixture for PCR (20 μl) contained approximately 250 ng of DNA, 67 mM Tris·HCl (pH 8.8), 16.6 mM $(NH_4)_2SO_4$, 0.45% Triton X-100, 200 μg of gelatin per ml, 1.5 mM $MgCl_2$, 250 μM of each dNTP, 12.5 ng of each primer, and 1.5 units of *Taq* polymerase. After initial denaturation (95°C for 150 s), 40 amplification cycles were performed (95°C for 50 s, 60°C for 50 s, and 72°C for 60 s). For Southern blot analysis, *Bgl* II-digested tail DNA was probed with a radiolabeled DNA fragment corresponding to GM-CSF genomic sequences deleted from the targeting construct (probe A) and was reprobed with probe B (Fig. 1) corresponding to sequences lying outside the targeting construct.

Mice. Chimeras from two independent ES cell clones with a disrupted GM-CSF gene transmitted the mutation in matings with C57BL/6 females. GM-CSF genotypic status was assessed by PCR analysis of tail DNA and is designated as follows: wild-type, GM+/+; heterozygous, GM+/−; and homozygous null, GM−/−. GM−/− mice were subsequently bred from GM−/− × GM−/− matings; similarly, outbred 129/OLA × C57BL/6 GM+/+ control mice were bred from first- and second-generation GM+/+ littermates. Mice were kept in a conventional animal house.

Spleen-Conditioned Media (SCM) and GM-CSF Assays. SCM were prepared (10) from splenocytes stimulated with concanavalin A (5 μg/ml; Boehringer Mannheim) and interleukin 2 (IL-2; 100 units/ml; Amgen Biologicals). To assay immunoreactive GM-CSF, an ELISA was used with the anti-GM-CSF antibody MP1-22E9 and biotinylated MP1-

The publication costs of this article were defrayed in part by page charge payment. This article must therefore be hereby marked "*advertisement*" in accordance with 18 U.S.C. §1734 solely to indicate this fact.

Abbreviations: G-CSF, M-CSF, and GM-CSF, granulocyte, macrophage, and granulocyte/macrophage colony-stimulating factors; SCM, spleen-conditioned media/medium; PAS, periodic acid/Schiff reagent (stain); IL-2, IL-3, and IL-6, interleukins 2, 3, and 6; SCF, stem cell factor; H&E, hematoxylin/eosin; ES cells, embryonal stem cells.

†Present address: National Institute for Medical Research, The Ridgeway, Mill Hill, London, NW7 1AA, United Kingdom.
‖To whom reprint requests should be addressed.

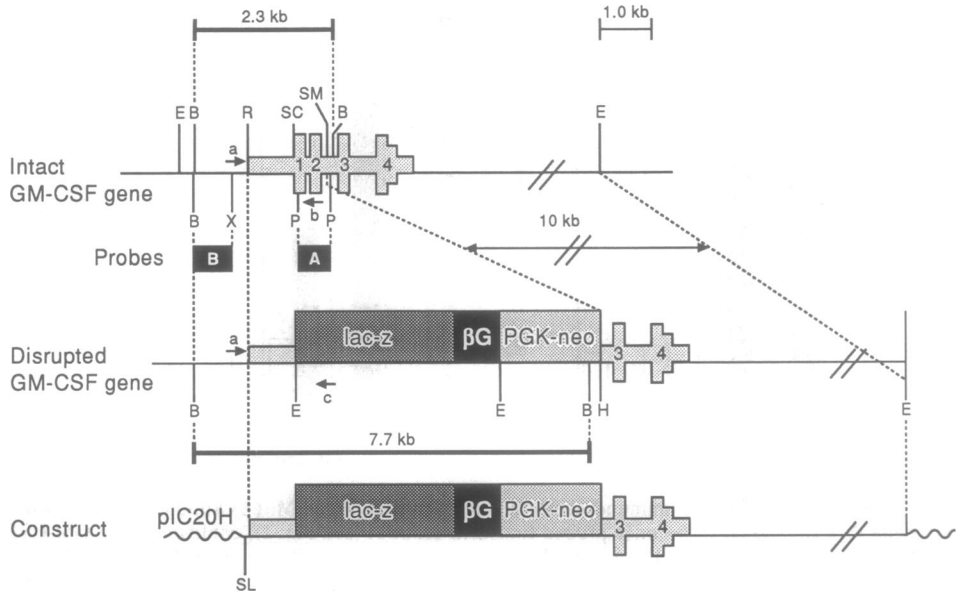

FIG. 1. Generation of GM-CSF deficient mice. Strategy for disruption of GM-CSF gene, showing intact and disrupted GM-CSF gene (exons labeled 1, 2, 3, and 4) and targeting construct, locations of restriction enzyme sites (E = *Eco*RI, B = *Bgl* II, SC = *Sca* I, SM = *Sma* I, X = *Xmn* I, P = *Pst* I, H = *Hin*dIII, SL = *Sal* I), probe A (corresponding to deleted sequences), probe B (external to construct, diagnostic for targeted disruption), and sites of PCR primer hybridization (**a**, **b**, and **c**; see text). In the disrupted allele, exons 1 and 2 and intron 1 are deleted, replaced by the *E. coli lacZ* gene, human β-globin gene 3′ untranslated and poly(A) addition sequences (βG), and PGK-neo (see text).

31G6 (PharMingen) with an avidin–biotinylated horseradish peroxidase (Dako) detection system (sensitivity, 50 pg/ml). To assay bioactive GM-CSF, the FDC-P1 proliferative response ([^{3}H]thymidine incorporation) was used with adjustment for interleukin 3 (IL-3) bioactivity on 32-D cells (11). The MP1-22E9 antibody was used to confirm specificity of putative GM-CSF bioactivity. Standards were recombinant murine GM-CSF (Schering–Plough) and IL-3 (10^7 units/mg; Boehringer Mannheim).

Immunohistochemistry and Electron Microscopy. Immunoperoxidase staining of lung tissue was performed on 4-μm frozen sections with the following antibodies (and specificity): RA3-6B2 (B220) (12), 187.1 (κ light chain) (13), GK1.5 (CD4) (14), 53.6-7 (CD8) (15), and 53-7.8 (CD5) (PharMingen). For electron microscopy, samples of fresh lung tissue were processed by standard techniques into Araldite–Epon resin, and thin sections were stained with alkaline lead citrate and uranyl acetate.

Hematological Analysis. Hemoglobin, total leukocyte, and platelet estimates were performed on 1:4 dilutions of eye-bleed samples with a Sysmex-K1000 automated counter; manual 100-cell leukocyte differential counts were performed on May–Grunwald/Giemsa-stained smears. Semisolid agar cultures of bone marrow, spleen, or peritoneal cells were prepared and scored as described (10, 16). Colony formation was stimulated by the following recombinant growth factors (at the specified final concentrations): human granulocyte colony-stimulating factor (G-CSF; 10 ng/ml), murine GM-CSF (10 ng/ml), murine IL-3 (10 ng/ml), murine macrophage colony-stimulating factor [M-CSF (CSF-1); 10 ng/ml], rat stem cell factor (SCF; 100 ng/ml), murine interleukin 6 (IL-6; 500 ng/ml), and SCM (10%).

Statistics. Data are given as means ± SD. To test for statistically significant differences, the unpaired Student *t* and χ^2 tests were used.

RESULTS

Verification of GM-CSF Gene Disruption. Southern blotting analysis of *Bgl* II-digested tail DNA confirmed the structure of the targeted allele in GM−/− mice: the 2.3-kb species hybridizing with the GM-CSF probe containing exons 1–2 was absent from GM−/− DNA, but GM−/− DNA contained the predicted 7.7-kb species hybridizing with the GM-CSF promoter probe external to the targeting vector (Fig. 2 *A*). GM−/− SCM contained no detectable immuno- or bioactive GM-CSF (Fig. 2 *A* and *B*), confirming the inability of GM−/− tissues to make GM-CSF. All GM−/− SCM were potent, containing bioactive IL-3, although GM−/− SCM contained less IL-3 than in GM+/+ SCM (GM−/− SCM, 16 ± 2 units/ml, $n = 4$; GM+/+ SCM, 49 ± 20 units/ml, $n = 4$; $P < 0.01$).

Viability and Fertility. From initial matings of GM+/− mice, litters of 10 ± 3 pups ($n = 8$) resulted with the genotypes GM+/+, GM+/−, and GM−/− represented in approximately Mendelian ratios, indicating no selective fetal or neonatal loss of GM−/− pups. Survival of GM−/− mice was normal [GM−/−, >91%, $n = 35$; GM+/+, >88%, $n = 17$) with the following median follow-up time: (range): GM−/−, 220 (0–334) days; GM+/+, 209 (0–313) days]. The two dead GM−/− mice in this cohort had lymphoid leukemia (died day 153) and the other had hepatitis (died day 167). From initial matings of male and female GM−/− mice, litters of 9 ± 1 pups ($n = 5$) resulted, indicating that GM-CSF deficiency did not grossly impair fertility or fecundity.

Hematological Analysis of GM-CSF-Deficient Mice. The peripheral blood of 6- to 7-wk GM−/− mice showed no significant difference from GM+/+ littermates. Respective values for GM+/+ ($n = 10$) and GM−/− ($n = 10$) mice were as follows: hemoglobin, 162 ± 7 and 163 ± 5 g/liter; platelets, 838 ± 105 × 10^9 and 822 ± 109 × 10^9 per liter; total leukocytes, 5.9 ± 1.0 × 10^9 and 7.4 ± 2.4 × 10^9 per liter; neutrophils, 1.1 ± 0.3 × 10^9 and 1.2 ± 0.6 × 10^9 per liter; lymphocytes, 4.7 ± 1.1 × 10^9 and 6.0 ± 2.0 × 10^9 per liter; monocytes, 0.12 ± 0.10 × 10^9 and 0.13 ± 0.13 × 10^9 per liter; and eosinophils, 0.09 ± 0.06 × 10^9 and 0.13 ± 0.13 × 10^9 per liter. GM−/− mice tended to have greater variation in their granulocyte levels [e.g., granulocyte levels of 5- to 7-wk mice were as follows: GM−/−, 1.7 ± 1.5 × 10^9 per liter ($n = 33$; range, 0.2–6.6); and GM+/+, 1.3 ± 0.7 × 10^9 per liter ($n = 15$; range, 0.29–3.1)]. Spleens of GM−/− mice showed increased variability in mass [e.g., spleen mass (range) of 6-wk mice, $n = 6$ per group, were as follows: GM+/+, 106 ± 9 (94–120) mg; and GM−/−, 114 ± 42 (64–191) mg]. Femoral cellularity was equivalent (GM+/+, 34.0 ± 5.3 × 10^6; and GM−/−, 27.4 ± 7.0 × 10^6 cells per femur, $n = 3$), and the myeloid:erythroid ratios were equivalent (20 ± 2% and 17 ± 6% erythroid cells, respectively). There was no major difference in marrow total progenitor cell frequency (Table 1), and colony typing indicated no differences in frequencies of granulocyte, granulocyte-macrophage, macrophage, eosinophil, megakaryocyte, erythroid, and blast marrow progenitor cells. In crowded unstimulated cultures of up to 2 × 10^5 GM−/− marrow cells per ml, colony formation

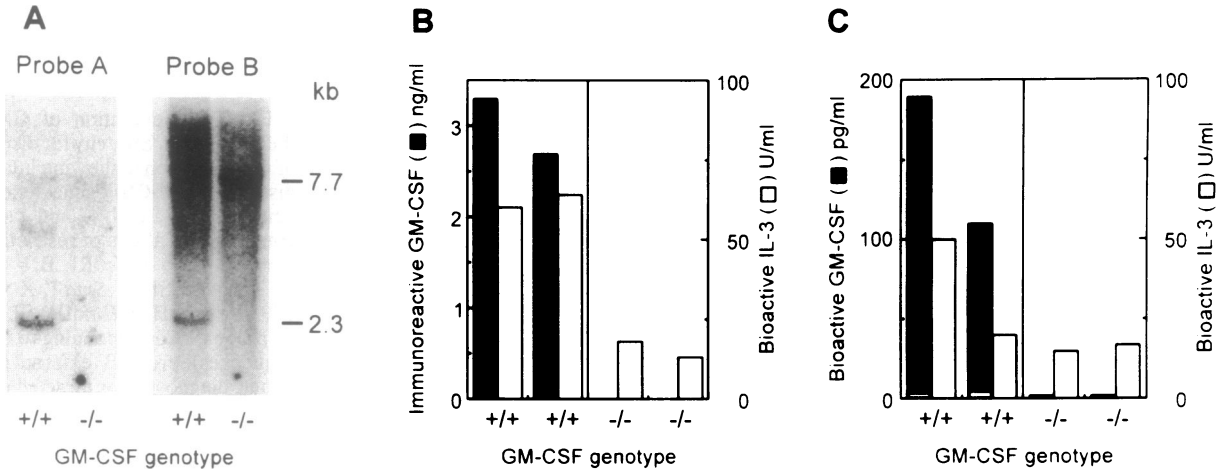

FIG. 2. Deletion of GM-CSF exons 1–2 results in lack of GM-CSF immunoreactivity and bioactivity in SCM. (*A*) Southern blot is shown of *Bgl* II-digested tail DNA from PCR-genotyped GM+/+ and GM−/− mice probed first with probe A (see Fig. 1), confirming that GM-CSF exons 1 and 2 are present in wild-type DNA but deleted from GM−/− DNA, and then reprobed with probe B, confirming that the GM−/− mouse is homozygous for the disrupted GM-CSF allele. (*B* and *C*) Levels of immunoreactive (*B*) and bioactive (*C*) GM-CSF (solid columns) and bioactive IL-3 (open columns) in media conditioned by concanavalin A- and IL-2-stimulated splenocytes are shown for individual GM+/+ and GM−/− mice. In *C*, the open portion of the solid column shows GM-CSF bioactivity after neutralization with an anti-GM-CSF antibody.

was only somewhat reduced, indicating that "spontaneous" colony formation *in vitro* is not solely dependent on GM-CSF production. There was a 3- to 6-fold increase in frequency of splenic progenitor cells in GM−/− mice and an absolute increase in splenic progenitor cell number (Table 1). Peritoneal washings recovered $6.0 \pm 1.4 \times 10^6$ and $5.1 \pm 1.4 \times 10^6$ cells from GM+/+ and GM−/− mice (65% and 63% macrophages, respectively).

Histological Characterization of Pulmonary Disease in GM-CSF-Deficient Mice. Although at birth the lungs of GM−/− and GM+/+ animals were indistinguishable, by 3 weeks of age striking abnormalities were evident. Individual GM−/− lungs consistently showed focal peribronchovascular aggregates of lymphoid cells but little infiltration of alveolar septa (Fig. 3 *A–C*). Immunostaining of 12- to 16-wk GM−/− lungs showed these cells to be predominantly B lymphocytes and about 20% T cells, predominantly $CD4^+$ (Fig. 3 *E–H*). The lymphoid infiltrate was particularly marked around hilar vessels, occasionally assuming a follicular organization, but the cells exhibited little mitotic activity. Characteristically, the perivascular infiltrate extended peripherally with a predilection for the perivascular area (Fig. 3*B*). Focal consolidation was prevalent, consisting of an eosinophilic alveolar exudate containing numerous mature and fragmented neutrophils and macrophages (Fig. 3*D*), occurring most commonly in the tips of lobes, but frequently was more extensive. In older 6- to 12-wk lungs, the lymphoid hyperplasia predominated, alveoli contained large foamy macrophages and granular debris, and focal acute inflammation sometimes occurred (Fig. 3*D*). One 6-wk GM−/− mouse had a chronic pulmonary abscess with an organized wall lined by foamy macrophages. Granular, eosinophilic, periodic acid/Schiff reagent (PAS)-positive, diastase-resistant material within alveoli was present in all lungs examined (3-wk- to 10-month-old mice) (e.g., Fig. 3 *D, K, O,* and *P*), apparently accumulating and becoming confluent in some alveoli. In some areas of GM−/− lungs, the appearances of contiguous alveoli containing this material resembled those of *alveolar proteinosis* (Fig. 3 *O* and *P*). Surfactant-producing type-II alveolar cells were readily identified by their cytoplasmic lamellar bodies (Fig. 4*A*); the alveolar debris included numerous type-C lamellar bodies (Fig. 4*B*), and these were seen within phagosomes of alveolar macrophages (Fig. 4*C*). Some alveolar spaces in older lungs were large, suggesting an emphysematous process (Fig. 3*Q*). One 4-wk-old GM−/− mouse died with lobar pneumonia (Fig. 3*N*) from which *Pasteurella pneumotropica* was isolated. Grocott and PAS stains identified foci of 5- to 10-μm-diameter fungal elements in 3 of 15 GM−/− lungs but in none of 7 GM+/+ lungs (e.g., Fig. 3 *I–K*). Gram-positive coccobacilli were present in one pneumonic area (Fig. 3 *L* and *M*). No mycobacterial infections were evident with Ziehl–Neelson and Wade–Fite stains.

Table 1. Hematopoietic progenitor cells in GM-CSF-deficient mice

Cells cultured, no.	*n*	Stimulus	Total colonies, mean ± SD GM+/+	GM−/−
Bone marrow				
25,000	5	GM-CSF	59 ± 12	51 ± 19
		G-CSF	19 ± 3	15 ± 7
		M-CSF	64 ± 16	59 ± 25
		IL-3	68 ± 12	68 ± 19
		SCF	29 ± 3	22 ± 13
		IL-6	18 ± 8	18 ± 10
		SCF + GM-CSF	66 ± 12	63 ± 26
200,000	5	Saline	79 ± 62	39 ± 44
Spleen				
100,000	3	GM-CSF	3 ± 4	8 ± 2
		SCF	0	4 ± 2*
		SCF + GM-CSF	3 ± 1	20 ± 2*
		SCM	4 ± 3	18 ± 2*

Genotype is indicated as wild-type (GM+/+) or GM-CSF-deficient (GM−/−). The spleen masses were 64 ± 8 mg for GM+/+ mice and 114 ± 22 mg for GM−/− mice ($P < 0.05$). *n* is the number of mice studied.
*$P < 0.05$.

DISCUSSION

Since the actions of hematopoietic regulators appear to overlap, it is possible that individual regulators might be wholly or partially redundant (5). This proposition is most directly assessed by analysis of mice deficient in individual or multiple regulators. Our analysis of GM−/− mice (up to 12 wk of age) indicates no perturbation of major hematopoietic populations in marrow or blood. There are two obvious interpretations: either GM-CSF may not be an important regulator of normal hematopoiesis, or alternatively, GM-CSF may contribute to the maintenance of steady-state he-

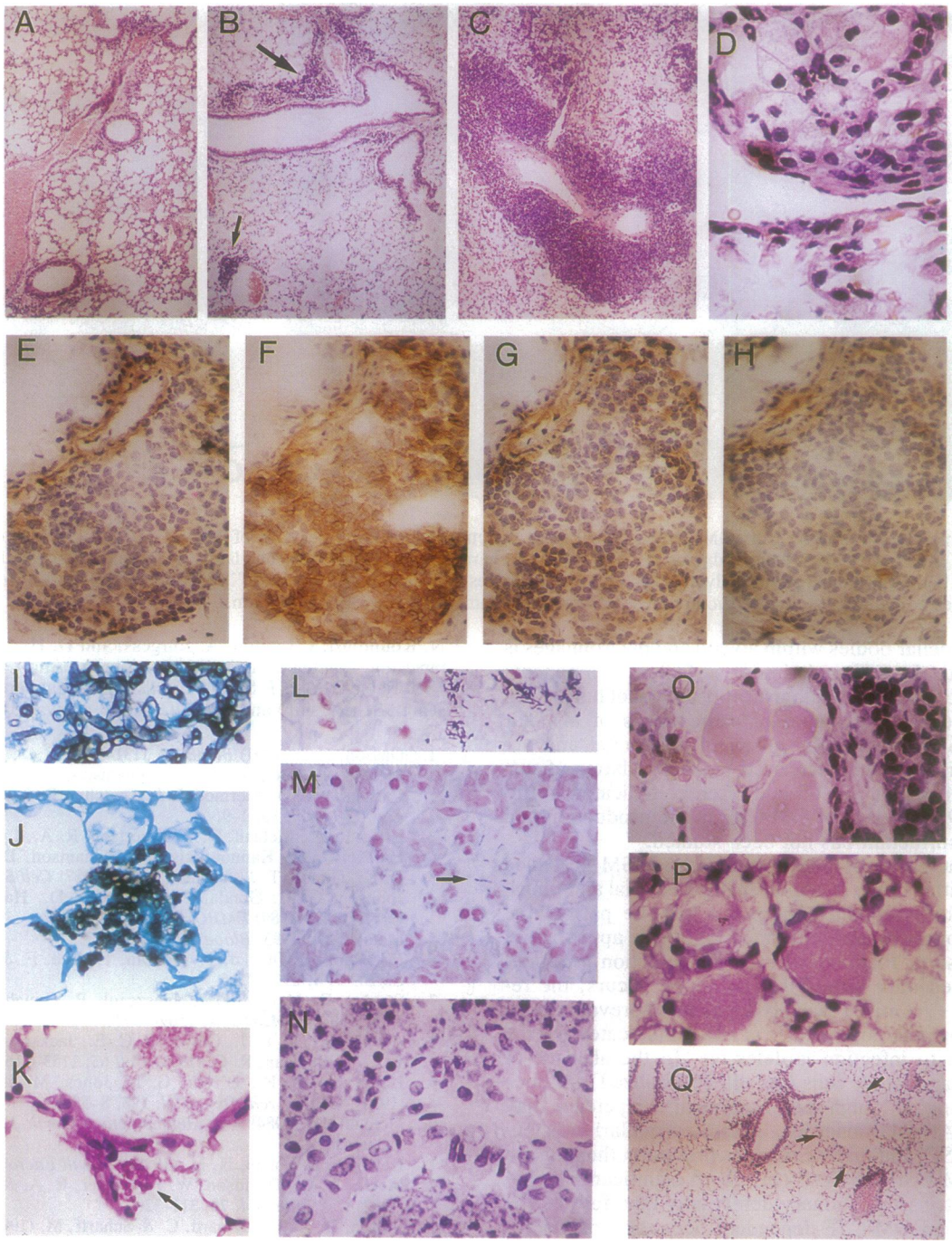

FIG. 3. Lung histopathology of GM-CSF-deficient mice. (*A*) Normal C57BL/6 lung (13 wk), central region. [Hematoxylin/eosin (H&E); ×20.] (*B* and *C*) GM−/− lung (11 wk) with moderate (*B*) and extensive (*C*) lymphoid hyperplasia around central and peripheral vessels. (H&E; ×20.) (*D*) Detail of alveoli in GM−/− lung (7 wk) with large foamy macrophages, neutrophils, and eosinophilic alveolar debris. (H&E; ×200.) (*E–H*) Immunoperoxidase staining of perivascular mononuclear cells in GM−/− mouse lung (16 wk) ×100 with the following primary antibodies (and specificity): none (phosphate-buffered saline; negative control) (*E*); RA3-6B2 (B220) (*F*); GK1.5 [CD4] (*G*); and 53.6-7 [CD8] (*H*). The same nodule is in each panel. (*E–H*, ×100.) (*I–K*) Focus of infection with fungal element in GM−/− lung (16 wk). (*I*) Positive control for Grocott stain. (*J*) Grocott-positive fungal particles of 5–10 μm. (*K*) PAS-positive fungal particles in same location of the contiguous section. (*I–K*, ×200.) (*L–N*) Bacterial infections in GM−/− lungs. (*L*) Gram stain control with Gram-positive and Gram-negative bacilli. (*M*) Gram-positive coccobacilli in 7-wk pneumonic consolidated area. (*N*) Purulent acute *Pasteurella pneumotropica* lobar pneumonia in mouse dying at 4 wk. (*N*, H&E; *L–N*, ×200.) (*O–Q*) Features of 24-wk GM−/− lung. (*O* and *P*) Granular refractile PAS-positive homogenous eosinophilic material in contiguous alveoli. (*Q*) Emphysematous area (e.g., arrow) with persistent peribronchovascular lymphoid hyperplasia. (H&E in *O* and *Q*, PAS in *P*; *O–Q*, ×200.)

matopoiesis, but in its absence other regulators are able to replace its usual role. Splenic progenitor cell levels were increased in GM−/− mice, but this may reflect subclinical pulmonary infection.

The possibility that GM-CSF is wholly redundant can be discounted because all GM−/− mice develop abnormal lungs. Our initial studies have not identified the nature of the intrinsic pulmonary defect that characterizes GM-CSF deficiency. The alveolar material that accumulates may be a local product, such as surfactant phospholipid and protein, either produced in excess or cleared too slowly possibly because of a functional defect of macrophages. The presence of numer-

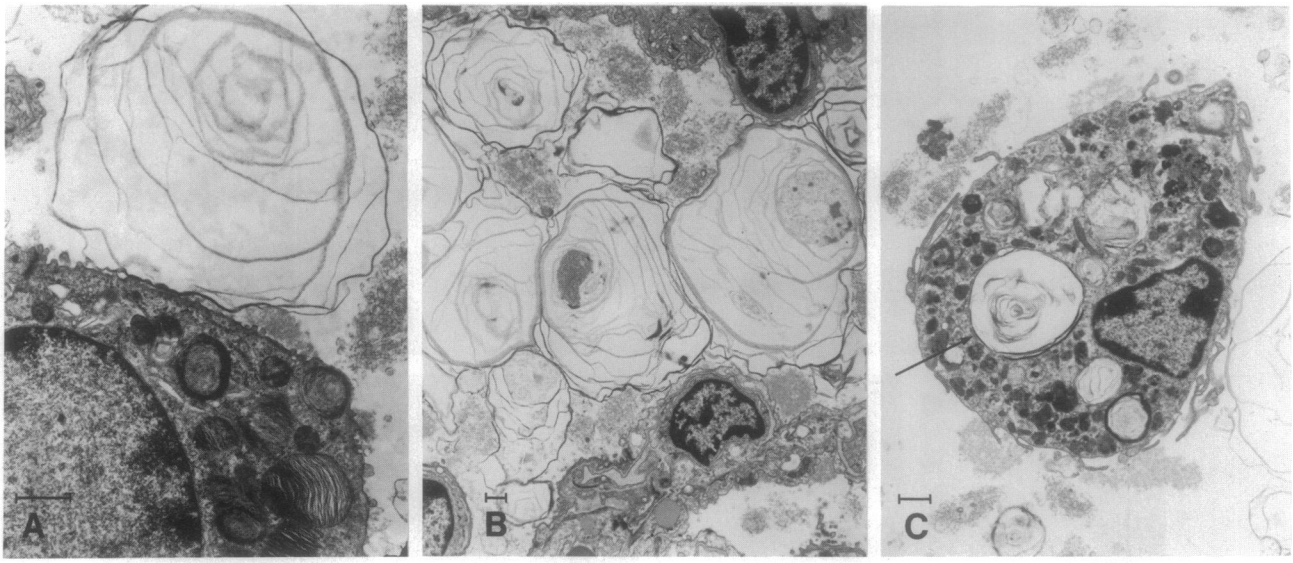

FIG. 4. Ultrastructure of lungs from GM-CSF-deficient mice. Electron microscopic sections of 24-wk GM−/− lung (same mouse lung as in Fig. 3 *O–Q*). (*A*) Type II surfactant-producing alveolar cell with characteristic intracytoplasmic lamellar bodies. Adjacent alveolus contains type-C lamellar body. (*B*) Numerous intraalveolar type-C lamellar bodies with characteristic "onion" appearance. (*C*) Intraalveolar macrophage with phagosomes containing "onion" structures resembling type-C lamellar bodies. (Bars = 1 μm.)

ous type-C lamellar bodies within alveoli and macrophages is consistent with the accumulation of surfactant components (17). In some areas, the histological appearance of lungs from GM−/− mice resembles that of some forms of alveolar proteinosis, a heterogeneous group of congenital and acquired lung disorders characterized by accumulation of surfactant protein within alveoli and often complicated by infection (17–19). The role of GM-CSF in the production and clearance of surfactant has not been studied.

A prominent feature of the lung pathology of GM−/− mice is infection with a range of opportunistic bacterial and fungal organisms. The lymphoid hyperplasia may be part of the general pulmonary response to infection; these appearances resemble those of *Pneumocystis carinii* infection in immunocompromised mice (20). When infection occurs, the response of GM−/− mice is usually adequate to prevent death, but the ongoing pathology in mice of all ages indicates that the host response to infection is defective. In the absence of GM-CSF, inflammatory cells can still be localized in tissues such as the lung, although their functional competence may be impaired. Alveolar macrophages are particularly responsive to GM-CSF, and many cell types present in the lung are capable of GM-CSF synthesis (21, 22). A significant component of the intrinsic pulmonary defect may therefore be the absence of local GM-CSF-dependent activation of macrophages involved in either surfactant clearance or infection control. It will be interesting to gauge the influence of environmental factors on both the hematologic and pulmonary manifestations of GM-CSF deficiency by comparing GM−/− mice raised in conventional and gnotobiotic animal facilities.

The pulmonary pathology accompanying absolute GM-CSF deficiency suggests therapeutic potential for GM-CSF in lung disorders characterized by infection or by the accumulation of alveolar material such as occurs in alveolar proteinosis. Acquired forms of alveolar proteinosis may reflect a local relative deficiency of GM-CSF. Among congenital forms of alveolar proteinosis, there may be a human counterpart to murine GM-CSF deficiency, for which GM-CSF replacement therapy would be appropriate.

We thank R. Williams, G. Mann, A. Gabriel, K. Fowler, J. Boyd, N. Kountouri, J. Layton, A. Burgess, and D. Henderson for assistance and comments on the manuscript. The Anti-Cancer Council of Victoria supported E.S. and G.J.L. (John Maynard Hedstrom Research Scholarship) and D.M. (Carden Fellowship Fund).

1. Gasson, J. C. (1991) *Blood* **77**, 1131–1145.
2. Metcalf, D., Begley, C. G., Williamson, D. J., Nice, E. C., De Larmarter, J. D., Mermod, J.-J., Thatcher, D. & Schmidt, A. (1987) *Exp. Hematol.* **15**, 1–9.
3. Lang, R. A., Metcalf, D., Cuthbertson, R. A., Lyons, I., Stanley, E., Kelso, A., Kannourakis, G., Williamson, D. J., Klintworth, G. K., Gonda, T. J. & Dunn, A. R. (1987) *Cell* **51**, 675–686.
4. Johnson, G. R., Gonda, T. J., Metcalf, D., Hariharan, I. K. & Cory, S. A. (1989) *EMBO J.* **8**, 441–448.
5. Metcalf, D. (1993) *Blood* **82**, 3515–3523.
6. Miyatake, S., Otsuka, T., Yokota, T., Lee, F. & Arai, K. (1985) *EMBO J.* **4**, 2561–2568.
7. Stanley, E., Metcalf, D., Sobieszczuk, P., Gough, N. M. & Dunn, A. R. (1985) *EMBO J.* **4**, 2569–2573.
8. Tybulewicz, V. L. J., Crawford, C. E., Jackson, P. K., Bronson, R. T. & Mulligan, R. C. (1991) *Cell* **65**, 1153–1163.
9. Handyside, A. H., O'Neil, G. T., Jones, M. & Hooper, M. L. (1989) *Roux's Arch. Dev. Biol.* **198**, 8–55.
10. Metcalf, D. (1984) *The Hemopoietic Growth Factors* (Elsevier, Amsterdam).
11. Kelso, A. & Gough, N. M. (1989) *Growth Factors* **1**, 165–177.
12. Morse, H. C., Davidson, W. F., Yetter, R. A. & Coffman, R. L. (1982) *Cell Immunol.* **70**, 311–320.
13. Yelton, D. E., Desaymard, C. & Scharff, M. (1981) *Hybridoma* **1**, 5–11.
14. Dialynas, D. P., Quan, Z. S., Wall, K. A., Pierres, A., Quintans, J., Loken, M. R., Pierres, M. & Fitch, F. W. (1983) *J. Immunol.* **131**, 2445–2451.
15. Ledbetter, J. A. & Herzenberg, L. A. (1989) *Immunol. Rev.* **49**, 63–90.
16. Metcalf, D. (1991) *Proc. Natl. Acad. Sci. USA* **88**, 11310–11314.
17. Shelburne, J. D., Wisseman, C. L., Broda, K. R., Roggli, V. L. & Ingram, P. (1983) in *Diagnostic Electron Microscopy*, eds. Trump, B. F. & Jones, R. T. (Wiley, New York), Vol. 4, pp. 475–532.
18. Rosen, S. H., Castleman, B. & Liebow, A. A. (1958) *N. Engl. J. Med.* **258**, 1123–1142.
19. Nogee, L. M., De Mello, D. E., Dehner, L. P. & Colten, H. R. (1993) *N. Engl. J. Med.* **328**, 406–410.
20. Beck, J. M., Warnock, M. L., Curtis, J. L., Sniezek, M. J., Arraj-Peffer, S. M., Kaltreider, H. B. & Shellito, J. E. (1991) *Am. J. Respir. Cell Mol. Biol.* **5**, 186–197.
21. Bilyk, N. & Holt, P. G. (1993) *J. Exp. Med.* **177**, 1773–1777.
22. Smith, S. M., Lee, D. K. P., Lacy, J. & Coleman, D. L. (1990) *Am. J. Respir. Cell Mol. Biol.* **2**, 59–68.